

## Mean value modelling of diesel engine combustion based on parameterized finite stage cylinder process

Sui, Congbiao; Song, Enzhe; Stapersma, Douwe; Ding, Yu

**DOI**

[10.1016/j.oceaneng.2017.03.029](https://doi.org/10.1016/j.oceaneng.2017.03.029)

**Publication date**

2017

**Document Version**

Accepted author manuscript

**Published in**

Ocean Engineering

**Citation (APA)**

Sui, C., Song, E., Stapersma, D., & Ding, Y. (2017). Mean value modelling of diesel engine combustion based on parameterized finite stage cylinder process. *Ocean Engineering*, 136, 218-232. <https://doi.org/10.1016/j.oceaneng.2017.03.029>

**Important note**

To cite this publication, please use the final published version (if applicable). Please check the document version above.

**Copyright**

Other than for strictly personal use, it is not permitted to download, forward or distribute the text or part of it, without the consent of the author(s) and/or copyright holder(s), unless the work is under an open content license such as Creative Commons.

**Takedown policy**

Please contact us and provide details if you believe this document breaches copyrights. We will remove access to the work immediately and investigate your claim.

# Title Page

1  
2  
3  
4  
5  
6  
7  
8  
9  
10  
11  
12  
13  
14  
15  
16  
17

## 1. Title

Mean value modelling of Diesel engine combustion based on parameterized finite stage cylinder process

## 2. Authors and Affiliations

Congbiao Sui<sup>1,2</sup>, Enzhe Song<sup>1</sup>, Douwe Stapersma<sup>2</sup>, Yu Ding<sup>1,\*</sup>

<sup>1</sup>College of Power and Energy Engineering, Harbin Engineering University, Harbin, China

<sup>2</sup>Faculty of Mechanical, Maritime and Materials Engineering, Delft University of Technology, The Netherlands

## 3. Corresponding author's complete contact information

\*Corresponding author: Yu Ding

● *Mailing address:* Room912, Power Building, College of Power and Energy Engineering, Harbin Engineering University, No. 145, Nantong Street, 150001, Harbin, China

● *Fax:* 0086 451 82589370

● *Telephone:* 0086 451 82589370

● *E-mail:* dingyu@hrbeu.edu.cn

## Highlights

18  
19  
20  
21  
22  
23  
24  
25  
26

1. Mean Value First Principle (MVFP) model has been built based on Seiliger process, i.e. the in-cylinder process of the engine is characterized by using parameterized finite stages.
2. The expressions to calculate the combustion parameters have been obtained.
3. MVFP diesel engine model built in this paper has been applied to the simulation of a ship propulsion system.
4. The simulation results have shown the adaptability of the MVFP model to variable working conditions and the capability of being integrated into a large system.

# Mean value modelling of Diesel engine combustion based on parameterized finite stage cylinder process

Congbiao Sui<sup>1,2</sup>, Enzhe Song<sup>1</sup>, Douwe Stapersma<sup>2</sup>, Yu Ding<sup>1,\*</sup>

<sup>1</sup>College of Power and Energy Engineering, Harbin Engineering University, Harbin 150001, China

<sup>2</sup>Faculty of Mechanical, Maritime and Materials Engineering, Delft University of Technology, The Netherlands

**Abstract:** Mean value diesel engine models are widely used since they focus on the main engine performance and can operate on a time scale that is longer than one revolution, and as a consequence use time steps that are much longer than crank-angle models. Mean Value First Principle (MVFP) models are not primarily intended for engine development but are used for systems studies that are become more important for engine users. In this paper two new variants of Seiliger processes, which characterize the engine in-cylinder process with finite stages are investigated, in particular their ability to correctly model the heat release by a finite number of combustion parameters. MAN 4L20/27 engine measurements are used and conclusions were drawn which Seiliger variant should be used and how to model the combustion shape for more engines. Then expressions to calculate the combustion parameters have been obtained by using a multivariable regression fitting method. The mean value diesel engine model has been corrected and applied to the simulation of a ship propulsion system which contains a modern MAN 18V32/40 diesel engine in its preliminary design stage and the simulation results have shown the capability of the integration of MVFP model into a larger system.

**Keywords:** diesel engine; combustion process; mean value model; combustion parameter; modelling

## 1 Introduction

The diesel engine has nowadays been dominantly used as prime mover of medium and medium-large devices, such as truck driving, land traction, ship propulsion, electrical generation, etc., owing to its reliability and good efficiency. The in-cylinder process during which the fuel is combusted and work delivered is the most crucial part of the diesel engine working processes. The in-cylinder process of a diesel engine is extremely complex, due to the complicated changes of the mass, energy and composition of the working medium. Whether the in-cylinder process is conducted properly or not has direct influences on the power prediction, fuel economy and emission behaviour etc. of a diesel engine (Lino Guzzella., et al., 2010; Asprion, J., et al., 2013).

53 With the rapid development of testing and computing technology, the in-cylinder process of diesel engines has been  
54 investigated quite deeply and in considerable details. A great variety of diesel engine in-cylinder process models have been  
55 developed using different methods and with different levels of detail due to various research and application purposes.  
56 Generally, an in-cylinder process model with higher accuracy is more complex, requiring more input parameters, longer  
57 calculation time and always are more difficult to adapt to different engines operating conditions (Guan, C., et al., 2014;  
58 Payri, F., et al., 2011). When a large system in which a diesel engine works as a subsystem of the whole system, for instance,  
59 the ship propulsion system, ship power generating system, ship heat recovery system, diesel engine electronic control system  
60 etc., is modelled and investigated, an in-cylinder model with high accuracy and complexity is not necessary, otherwise the  
61 system model will have a poor real-time capability and a bad adaptability to variable operating conditions (Woodward J B,  
62 Latorre R G, 1984).

63 Mean value models of diesel engine in-cylinder process taking both simplicity and accuracy into consideration have  
64 been widely used in the modelling of large systems. The in-cylinder process *mean value* models focus on the main engine  
65 performance parameters such as the air-fuel ratio, maximum in-cylinder pressure and temperature, engine brake power, etc.,  
66 rather than the in-cycle variations with steps of a crank angle (Theotokatos G, 2010). Mean value models have been  
67 extensively applied in the investigation of the transient behaviour of diesel engine and simulation at system level due to  
68 their simplicity and sufficient accuracy (Murphy, A. J., et al., 2015). Much research on mean value modelling of diesel  
69 engines has been conducted using different approaches, such as the regression-based and the thermodynamics-based mean  
70 value models. Regression-based mean value models have inherent limitations just predicting the input-output relationships  
71 and neglecting the underlying physical and thermodynamic process of the diesel engine, due to their heavy dependence on  
72 the regression analysis of the experimental data (Moskwa, J., et al., 1992; Kao, M., et al., 1995). Thermodynamic-based  
73 mean value models are derived from the basic physics and thermodynamics which can predict the physical and  
74 thermodynamic causalities of the engine working processes rather than algebraic equations just representing the  
75 input-output relationships (Maftei, C., et al., 2009; Lee, B., et al., 2013; Grimmelius, H.G. et al, 2007; Miedema, S., et al.,  
76 2002).

77 Mean value models of diesel engine that were applied for modelling of marine diesel engines and simulation of ship  
78 propulsion system have been extensively reported in the published scientific literature. Theotokatos (Theotokatos, G. P.,  
79 2008) has investigated the transient response of a ship propulsion plant using a mean value engine model. Vrijdag (Vrijdag  
80 A., et al., 2010) has applied the diesel engine model for the control of propeller cavitation in operational conditions. Baldi,  
81 F (Baldi, F., et al., 2015) has developed a mean value diesel engine model that has been used to investigate the propulsion

82 system behaviour of a handymax size product carrier for constant and variable engine speed operation. Michele Martelli  
83 (M Martelli, 2014) has developed a ship motion model taking into account all six degrees of freedom and a propulsion  
84 plant model that includes the mean value model of the diesel engine. In these models at system level, it is generally  
85 sufficient to predict the global behaviour of the engine and it is less important and unnecessary to investigate the engine  
86 thermodynamics deeply (Altosole, M. and M. Figari, 2011).

87 The thermodynamic-based MVFP models were originally developed by Delft University of Technology (TU Delft,  
88 the Netherlands) and Netherlands Defence Academy (Grimmelius, H., et al., 2007). A MVFP model of diesel engine MAN  
89 L58/64 has been built based on the basic five-point Seiliger process by Miedema (Miedema, S., et al., 2002), and the  
90 simulation results have shown the behaviour of a few important parameters in the dynamic process. Schulten (Schulten  
91 PJM, 2005; Grimmelius, H., et al., 2007) has built a MVFP diesel engine model based on the basic six-point Seiliger  
92 process and has used the engine model to investigate the interaction between diesel engine, ship and propeller during  
93 manoeuvring.

94 In this paper, firstly, a thermodynamic-based MVFP diesel engine model based on the *advanced* six-point Seiliger  
95 cycle will be introduced and the systematic investigation of the combustion parameters under various operating conditions  
96 will be presented based on MAN 4L20/27 diesel engine measurements. Then a MVFP model of MAN 4L20/27 that is built  
97 based on the *basic* six-point Seiliger cycle will be shown. The combustion parameters mathematical models of the MVFP  
98 model are derived by multiple regression analysis of experimental data and are validated. The model originally built for the  
99 diesel engine MAN 4L20/27 are then corrected and used to model diesel engine MAN 18V32/40, after which the engine  
100 mean value model has been applied to the simulation and performance prediction of the propulsion system of a large  
101 semi-submersible heavy lift vessel (SSHLV) during its preliminary design stage in order to verify the integration of the  
102 MVFP model into a larger system. The results of the mean value diesel engine modelling and application will be analysed.

## 103 **2 Model description and measurement investigation**

### 104 **2.1 Characterization of the in-cylinder process**

105 The diesel engine in-cylinder process can be parameterized by finite stages in different kinds of Seiliger processes,  
106 providing a simple and reliable method for mean value modelling of the cylinder process. Often the 5-point Seiliger process  
107 with two combustion stages is used (Dual Cycle) but in order to model combustion adequately a 6-point Seiliger process  
108 offering 3 or 4 stages of combustion is deemed necessary here.

109 2.1.1 Six-point Seiliger cycle

110 In this paper both the basic and advanced 6-point Seiliger cycles are investigated. Fig.1 shows the six-point Seiliger  
 111 process model. The stages can be described as follows:

112 1-2: polytropic compression;

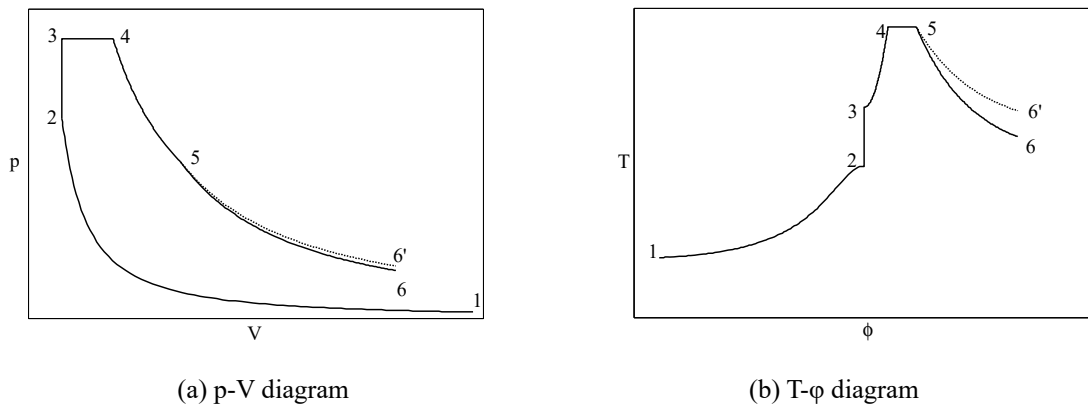
113 2-3: isochoric combustion;

114 3-4: isobaric combustion and expansion;

115 4-5: isothermal combustion and expansion;

116 5-6: polytropic expansion indicating a net heat loss, used when there is no combustion in this stage (basic);

117 5-6': polytropic expansion indicating a net heat input caused by late combustion during expansion (advanced).



120 **Fig.1** six-point Seiliger process definition [Ding Y, 2011]

121 2.1.2 Parameterization of the in-cylinder process

122 The Seiliger process can be described by a finite number of parameters that fully specify the process together with  
 123 the initial (trapped) condition and the working medium properties.

124 The definition of the Seiliger stages and the Seiliger parameters are given in Table 1. Among these Seiliger  
 125 parameters  $a$ ,  $b$  and  $c$  are the combustion parameters indicating the isochoric combustion stage, isobaric combustion stage  
 126 and isothermal combustion stage respectively. The polytropic compression exponent  $n_{comp}$  and effective compression ratio  
 127  $r_c$  model the polytropic compression process while the polytropic expansion exponent  $n_{exp}$  and expansion ratio  $r_e$  model  
 128 the polytropic expansion process.

129 **Table 1** Seiliger process definition and parameters

Seiliger stage	Seiliger definition	Parameter definition	Seiliger parameters
1-2	$\frac{p_2}{p_1} = r_c^{n_{comp}}$	$\frac{V_1}{V_2} = r_c$	$r_c, n_{comp}$

2-3	$\frac{V_3}{V_2} = 1$	$\frac{p_3}{p_2} = a$	$a$
3-4	$\frac{p_4}{p_3} = 1$	$\frac{V_4}{V_3} = b$	$b$
4-5	$\frac{T_5}{T_4} = 1$	$\frac{V_5}{V_4} = c$	$c$
5-6 (5-6')	$\frac{p_5}{p_6} = r_e^{n_{exp}}$	$\frac{V_6}{V_5} = r_e$	$r_e, n_{exp}$

**Table 2** Work and Heat in Seiliger process

Seiliger stage	Work $W$ [J]	Heat $Q$ [J]
1-2	$W_{12} = m_{12} \cdot \frac{R_{g,12}}{n_{comp} - 1} \cdot (T_1 - T_2)$	$Q_{12} = m_{12} \cdot \frac{\kappa_{12} - n_{comp}}{n_{comp} - 1} \cdot c_{v,12} \cdot (T_2 - T_1)$
2-3	$W_{23} = 0$	$Q_{23} = m_{23} \cdot c_{v,23} \cdot (T_3 - T_2)$
3-4	$W_{34} = m_{34} \cdot R_{g,34} \cdot (T_4 - T_3)$	$Q_{34} = m_{34} \cdot c_{p,34} \cdot (T_4 - T_3)$
4-5	$W_{45} = m_{45} \cdot R_{g,45} \cdot T_4 \cdot \ln\left(\frac{V_5}{V_4}\right)$	$Q_{45} = m_{45} \cdot R_{g,45} \cdot T_4 \cdot \ln\left(\frac{V_5}{V_4}\right)$
5-6 (5-6')	$W_{56} = m_{56} \cdot \frac{R_{g,56}}{n_{exp} - 1} \cdot (T_5 - T_6)$	$Q_{56} = m_{56} \cdot \frac{n_{exp} - \kappa_{56}}{n_{exp} - 1} \cdot c_{v,56} \cdot (T_6 - T_5)$

130

131

132

133

134

135

136

137

138

139

For a certain engine  $r_c$  which depends on the geometry of the combustion chamber and the timing of inlet valve closing (IC) can be set as constant.  $n_{comp}$  can also be regarded as constant during the compression process under various operating conditions according to the real process.  $r_e$  depends on  $b$  and  $c$  and the timing of the exhaust valve opening (EO), only the latter being constant.  $n_{exp}$  is assumed to be constant for the basic Seiliger process (but like  $a$ ,  $b$ , and  $c$  is a variable for the advanced Seiliger process. Once all the Seiliger parameters are known, the pressures, temperatures, work and heat in the various stages of the Seiliger cycle can be calculated according to Table 1 and Table 2.

Seiliger processes can be categorized into various types as shown in Table 3 according to the total number of in-cylinder process stages and the number of combustion stages. (Ding Y, 2011).

**Table 3** Summary of Seiliger process models

In-cylinder process stage	Combustion stages	Parameters used for combustion	Theoretical investigation	Modelling application
5	2	$a, b$	Ref (Stapersma D, Woud H K, 2002; Miedema, S., et al., 2002)	Ref (Miedema, S., et al., 2002)
6	3	$a, b, c$	Ref (Schulten PJM, 2005; Grimmeliu, H., et al., 2007)	Ref (Schulten PJM, 2005; Grimmeliu, H., et al., 2007), improved in this paper
6	4	$a, b, c, n_{exp}$	Ref (Ding Y, 2011), improved in this	Prime investigation in this paper.



In-cylinder process stage	Combustion stages	Parameters used for combustion	Theoretical investigation	Modelling application
paper				

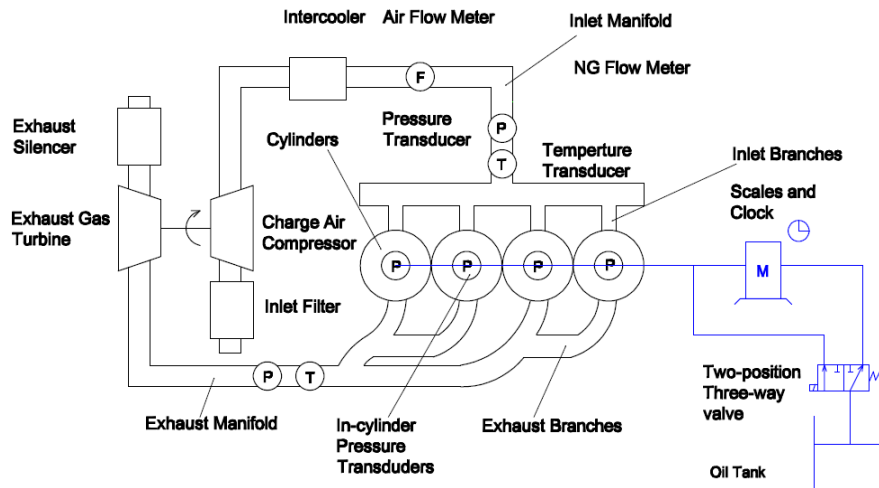
## 140 2.2 Experimental investigation of the Seiliger combustion parameters

141 In this section an experimental investigation of the Seiliger combustion parameters is carried out, based on diesel  
 142 engine measurements. The Seiliger combustion parameters are obtained based on the test data of a MAN 4L20/27 diesel  
 143 engine using curve fitting method. The main specifications of the MAN 4L20/27 diesel engine are shown in Table 4.

144 Fig. 3 illustrates the engine test bed layout. The in-cylinder pressure sensors, inlet pressure and temperature sensors,  
 145 exhaust pressure and temperature sensors, air flow meters, etc. are installed at the corresponding positions of the test  
 146 bed respectively. A weighing machine and clock with a two-position three-way valve instead of a flow meter have been  
 147 used for the fuel flow measurement, which is a traditional method but ensures the accuracy of the fuel flow  
 148 measurement.

149 **Table 4** Main specifications of diesel engine MAN 4L20/27

Parameter	Unit	Value
Nominal Engine Speed	rpm	1000
Maximum Effective Power	kW	340
Cylinder Number	-	4
Bore	m	0.20
Stroke	m	0.27
Compression Ratio	-	13.4
Connection Rod Length	m	0.52
Fuel Injection		Plunger pump Direct injection
Start of Injection	deg	4°before TDC
Inlet Valve Close	deg	20°after BDC
Outlet Valve Open	deg	300°after BDC



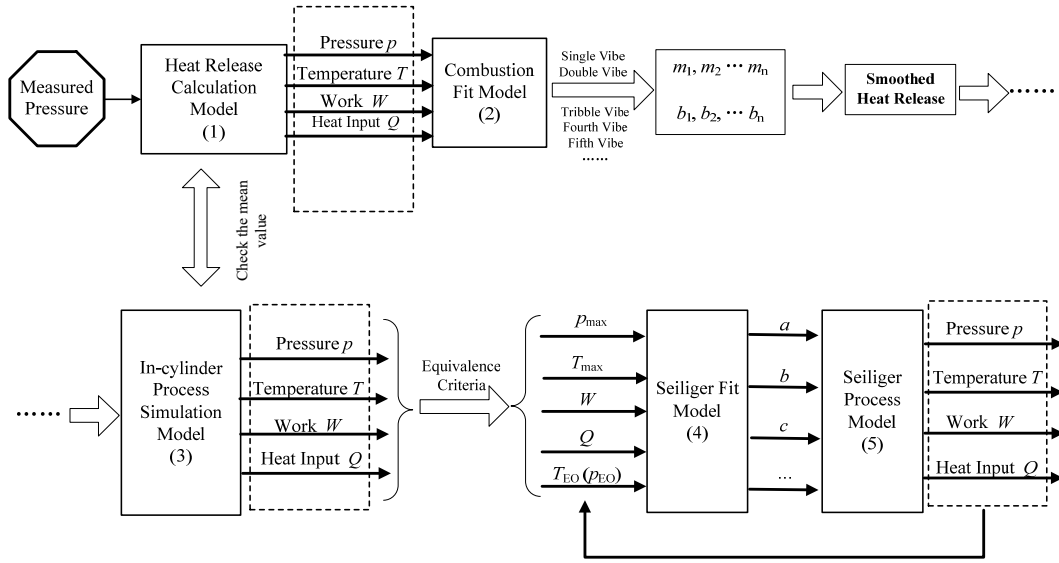
150  
151 **Fig.2** Schematic diagram of in-cylinder pressure measurement test bed

152 Fig. 3 shows the flow chart of a Seiliger fit simulation based on the measured in-cylinder pressure. The simulation  
153 procedure involves five main sub-models: 1) heat release calculation model; 2) Vibe combustion fit model; 3)  
154 in-cylinder process simulation model; 4) Seiliger fit model and 5) Seiliger process model. The prime input of the  
155 procedure is the measured in-cylinder pressure and the output is the Seiliger combustion parameters. The complete  
156 procedure as developed by Ding Yu (Ding Y, 2011) will briefly be summarised here.

157 The ‘heat release calculation’ model uses measured data, primarily the in-cylinder pressure, to calculate the  
158 reaction rate according to the ‘first law of thermodynamics’ and the in-cylinder temperature based on the ‘ideal gas law’.  
159 The latter is normal practice (Heywood, 1988) and the deviations from real gas behaviour are small (Lapuerta, M., et al,  
160 2006). The combustion reaction rate (CRR), which is in fact the output of the ‘heat release calculation’ model, is  
161 integrated to get the monotonous increasing and smoother reaction co-ordinate (RCO), which then can be corrected to  
162 fit the gross heat input. The ‘combustion fit model’ makes use of multiple Vibe functions. The multiple Vibe parameters  
163 fitted with the ‘combustion fit model’ are then the inputs of the ‘in-cylinder process simulation model’, in which the  
164 major in-cylinder parameters can be obtained. Then the Seiliger parameters are determined on the basis of a chosen  
165 combination of equivalence criteria between Seiliger process and in-cylinder process of the real engine. The Seiliger  
166 combustion parameters are calculated from the ‘Seiliger fit model’. This iteration method uses the equivalence  
167 parameters that are calculated by the ‘Seiliger process model’. Finally the in-cylinder behaviour is expressed by the  
168 Seiliger combustion parameters, which characterize the cylinder process and in particular the ‘combustion shape’.

169 With the simulation procedure, the Seiliger combustion parameters can be calculated for a wide range of operating  
170 conditions of the diesel engine. After obtaining the Seiliger combustion parameters for all measured points over the  
171 engine operational map, their trend as function of the engine operating conditions can be presented. In this paper, one

172 operating point at the propeller curve, i.e. 80% nominal speed and 50% nominal effective power of the engine, is  
 173 selected for the analysis.

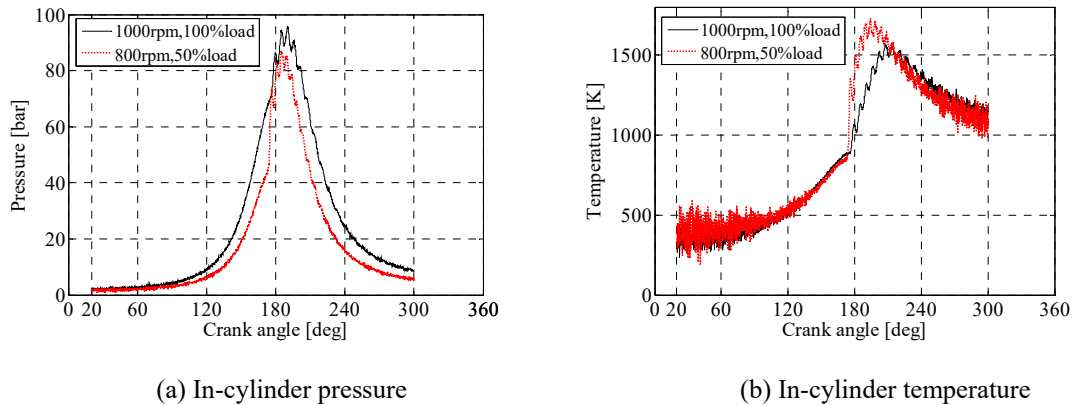


174  
 175 **Fig. 3** Flow chart of the overall simulation procedure to calculate Seiliger parameters, ref to (Ding Y, 2011)

176 *2.2.1 Heat Release Calculation and Pressure Smoothing*

177 The in-cylinder gas state parameters, namely in-cylinder pressure and temperature, are shown in Fig. 4. The  
 178 pressure signals are derived from the measurement directly and the temperatures are calculated on the basis of the ‘ideal  
 179 gas law’. At first sight it seems that the fluctuations in temperature are much fiercer than that in pressure. Closer  
 180 inspection reveals that the fluctuations relative to the instantaneous values are identical for pressure and temperature as  
 181 expected from the gas law. The effect is a graphical effect since the order of magnitude of the temperatures is much  
 182 larger relative to the maximum (i.e. 400 K versus 1300 K) than for the pressures (i.e. 1 bar versus 90 bars). The  
 183 differences between the two operating conditions are clearly revealed in these two figures.

184



185

186

187

**Fig. 4** In-cylinder pressure and temperature

188

189

190

191

192

193

194

195

196

197

198

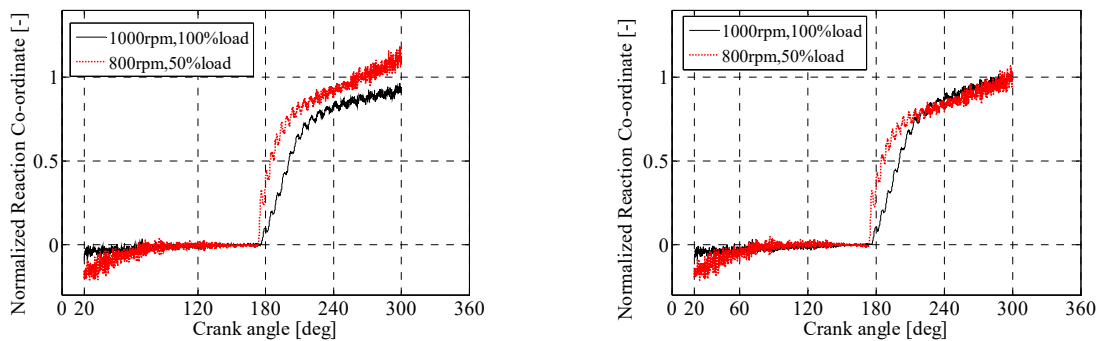
199

200

201

The Reaction coordinate (RCO) which is the integral of the Combustion Reaction Rate (CRR) is a monotonous increasing function, suitable for analysis and curve fitting as most of the fluctuations are smoothed in the integration process. Theoretically, the normalized reaction coordinate should reach unity for complete combustion. However, this is not a fixed value but the result of a rather complex calculation and often is not reached (see Fig. 5(a)). The heat loss is derived from the empirical Woschni equations (Woschni, 1967), resulting in uncertainty when calculating the reaction coordinate. Overrating or underrating the heat loss to the walls could lead to a final normalized reaction coordinate being above or below unity. Therefore the constants in Woschni equations are considered varying parameters that can be used to bring the RCO to unity at different operating points, as shown in Fig. 5(b). After correcting the RCO by adjusting the constants in the Woschni equations specifically to different operating points, the RCO after the start of combustion (SOC) is reasonable, however, the RCO before SOC gives unrealistic values. The RCO during the initial stages, in particular at the beginning of the in-cylinder process, is negative, which seems to an endothermic process at the beginning of the cycle. The negative values of the RCO during the initial in-cylinder process could still be caused by the estimation of heat loss as well as by the start value of RCO but most probably are just caused by the poor quality of the pressure signal at low pressure levels.

202



203

(a) Combustion Reaction co-ordinate (original)      (b) Combustion Reaction co-ordinate (corrected)

204

**Fig. 5** Combustion Reaction co-ordinate

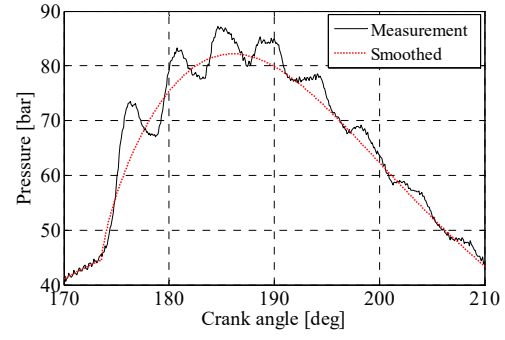
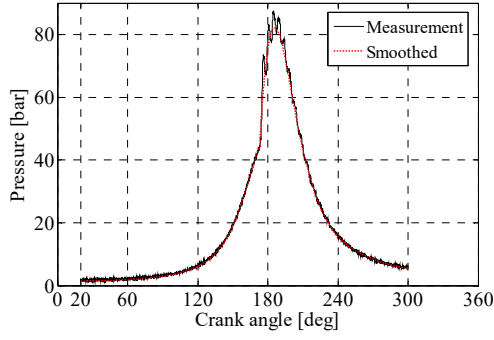
205

206

207

208

The erratic in-cylinder pressure signals measured from the engine test facilities need to be smoothed before being used to fit the Seiliger process model. In this paper, the pressure signals smoothing method presented in (Ding Y et al., 2011), which uses not only mathematic calculation but also thermodynamics knowledge, is followed. Fig. 6 shows the smoothed in-cylinder pressure signals along with the zoom in area of the peak pressure.



(a) In-cylinder pressure signals

(b) In-cylinder pressure signals (zoom in)

**Fig. 6** Smoothed in-cylinder pressure signals

### 2.2.2 Seiliger Process Fitting

The fit results of the engine operating point at 1000 rpm and 25% nominal power along the generator curve are presented in this section.

When the Seiliger process is fitted to a measured cycle, the number of finite combustion stages determines the number of features, i.e. the equivalence criteria, which can be made equal for the measured cycle and the Seiliger model cycle (Ding, Y., et al., 2012). In this paper, four equivalence criteria relate the Seiliger process to the measured engine parameters that are deemed important. Therefore they should be selected to cover the engine performance as fully as possible. Significant in-cylinder quantities, namely  $p_{max}$ ,  $W_i$ ,  $Q_{in}$ , and  $T_{max}$  are selected to calculate the four Seiliger parameters, i.e.  $a$ ,  $b$ ,  $c$  and  $n_{exp}$ , by equations (1) to (4) consociated with Table 1 and Table 2. The other Seiliger parameters are set to the base value as shown in Table 5. The calculation results as well as the error analysis are shown in Table 5.

$$p_{max} = p_1 \cdot r_c^{n_{comp}} \cdot a \quad (1)$$

$$T_{max} = T_1 \cdot r_c^{n_{comp}-1} \cdot a \cdot b \quad (2)$$

$$Q_{in} = Q_{23} + Q_{34} + Q_{45} + Q_{56} \quad (3)$$

$$W_i = W_{12} + W_{23} + W_{34} + W_{45} + W_{56} \quad (4)$$

**Table 5** Results of fitted Seiliger parameters

Seiliger parameters		Value	EC*	Relative Error (%)	Difference <sup>&amp;</sup>	
					Absolute	Relative
Constant	$n_{comp}$	1.36				
	$r_c$	13.1073				
Variable	$a$	1.5281	$p_{max}$	0		
	$b$	1.0445	$W_i$	0.1049		
	$c$	1.0996	$Q_{in}$	$7.014 \times 10^{-2}$		
	$n_{exp}$	1.3185	$T_{max}$	$8.475 \times 10^{-4}$		
			$T_{EO}$		-17.648 K	-1.67%

232

233 \* EC here means Equivalence Criterion

234 & the difference is the equivalence criterion of the Seiliger fit minus the value of the smoothed measurement

235 Table 6 illustrates the heat release  $Q_{56, ratio}$  in this operating point (1000 rpm, 25 % power) is 2.58% of the total net  
236 heat release. Also two other points at higher power are entered in Table 6 and then it is seen that the very late combustion  
237 can be significant, indicating that the heat input during this stage perhaps should not be neglected in this older engine. In  
238 modern engines with high-pressure injection and common rail systems one would not expect late combustion anymore.  
239 Later in the paper we will drop the very late combustion.

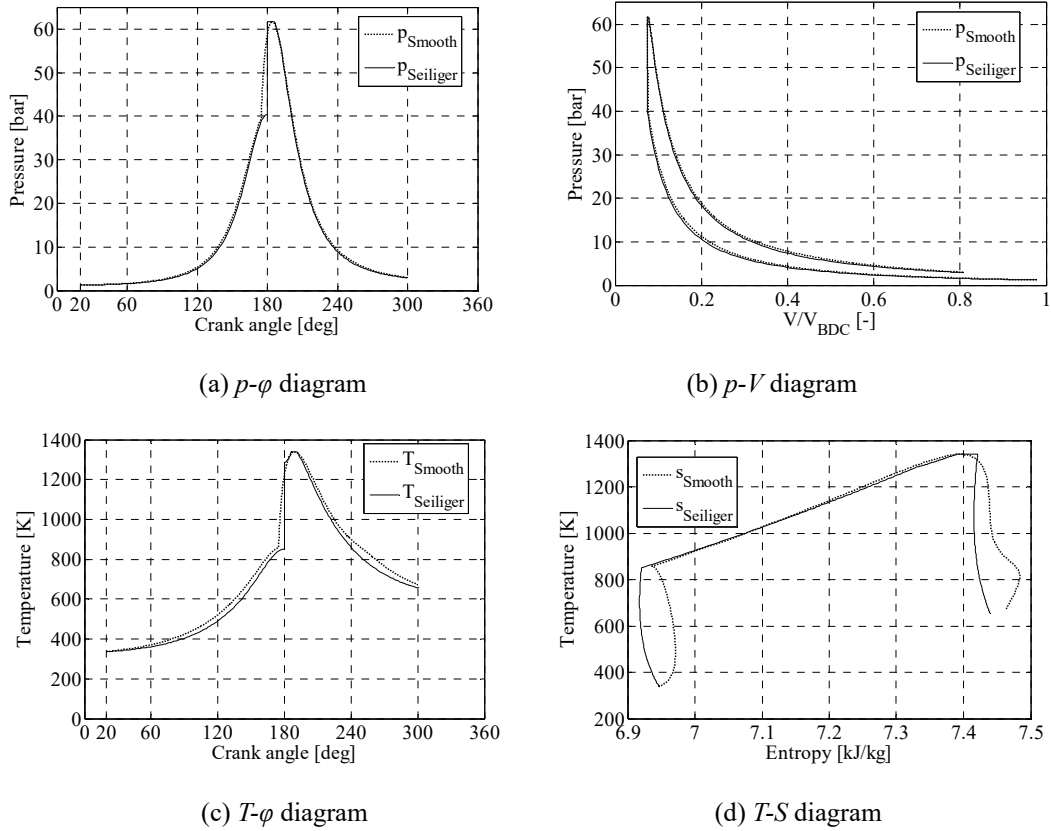
240

**Table 6** Heat input ratio of each stage at different operating points

	$Q_{23, ratio}$	$Q_{34, ratio}$	$Q_{45, ratio}$	$Q_{56, ratio}$
1000 [rpm] 25% power	0.7638	0.1343	0.0734	0.0258
1000 [rpm] 100% power	0.2080	0.4076	0.1042	0.2802
800 [rpm] 50% power	0.5300	0.1814	0.0917	0.1968

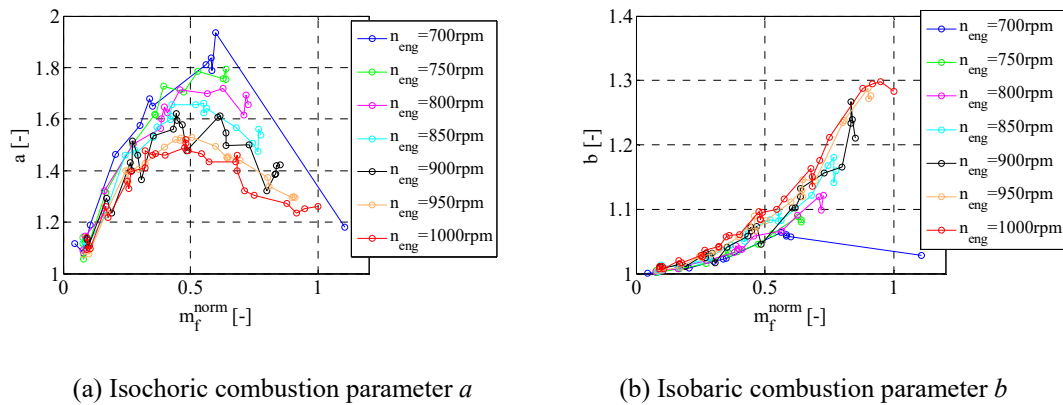
241 Fig. 7 shows the comparison of the fitted six-point Seiliger cycle with the smoothed measurement in four typical  
242 thermodynamic diagrams. In the smoothed measurement, a realistic heat transfer with the wall is calculated (using  
243 Woschni equations) i.e. first heating up and then cooling of the air in the cylinder. However, in the (theoretical) Seiliger  
244 cycle compression and expansion are polytropic processes with the parameters chosen such that cooling is the result,  
245 and the inclination of the T-S diagram is determined by the chosen polytropic exponents, specific heat and temperature.

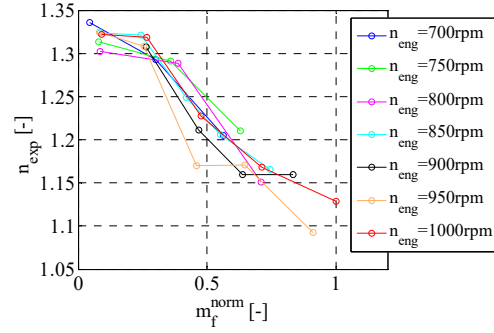
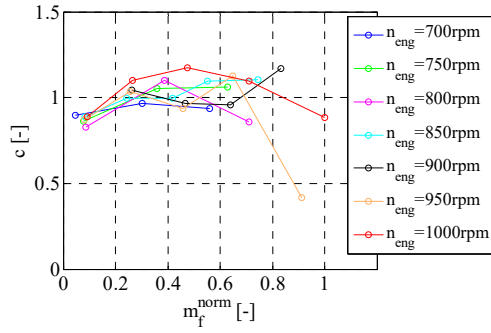
246 That's the reason why there are discrepancies between the smoothed measurement and the Seiliger curve in Fig. 7 (d).  
 247 Detailed explanations can be found in appendix V of (Ding Y, 2011).



252 **Fig. 7** Comparison of fitted Seiliger cycle with smoothed measurement

253 Only one operating point based on six-point Seiliger process is presented in this paper, but the Seiliger parameters as  
 254 function of engine rotational speed and fuel injection quantity have been investigated over a wide range of operating  
 255 conditions of the diesel engine. Fig.8(a) and Fig.8(b) show the relationship between combustion parameters and the  
 256 working condition parameters according to the test data of MAN 4L20/27. In the figures,  $m_f^{norm}$  is the normalized fuel  
 257 mass as shown in equation (6).





(c) Isothermal combustion parameter  $c$

(d) Expansion combustion parameter  $n_{exp}$

**Fig.8** Relationships between combustion parameters and fuel mass at different engine speeds

Fig.8(c) and Fig.8(d) show the relationship between parameter  $c$  and  $n_{exp}$  in advanced Seiliger process and fuel mass at different engine speeds. When modelling the diesel engine in-cylinder process, if the three combustion stage model is used such as in the basic six-point Seiliger process model, only two combustion parameters needs to be modelled while the other is obtained by the total heat input minus the two stages already calculated. Likewise for the advanced Seiliger process three combustion parameters must be modelled and the fourth can be obtained from the total heat.

### 3 Combustion parameters calculation

In this part the mean value model of MAN 4L20/27 built based on the basic six-point Seiliger cycle will be presented. Operating conditions as defined by diesel engine rotational speed and fuel injection quantity have a significant influence on the combustion process, which can be modelled by the combustion parameters in the Seiliger cycle. In this paper, the functional relationships between operating condition parameters and combustion parameters have been investigated and regression formulas calculating the combustion parameters have been fitted based on the test data of the diesel engine MAN 4L20/27.

#### 3.1 Normalising the operating condition parameters

In this paper, both the engine speed and fuel mass injected into cylinders per cycle have been normalised, making the subsequent analysis and regression fitting more convenient and improving the generality of the regression formulas which calculate the combustion parameters, see equations (5) and (6). The formulas will be corrected and applied to model MAN 18V32/40.

$$n_{eng}^{norm} = \frac{n_{eng}}{n_{eng,nom}} \quad (5)$$



282

$$m_f^{norm} = \frac{m_f}{m_{f,nom}} \quad (6)$$

283

Where,

284

 $n_{eng}^{norm}$  is the normalized engine speed, -;

285

 $m_f^{norm}$  is the normalized fuel mass, -;

286

 $n_{eng}$  is the engine speed, rpm;

287

 $m_f$  is the fuel mass, g/cylinder/cycle;

288

 $n_{eng,nom}$  is the nominal engine speed, rpm;

289

 $m_{f,nom}$  is the nominal fuel mass, g/cylinder/cycle.

290

291

292

293

294

295

296

From Fig.8(a) and Fig.8(b), at each engine speed, the value of  $a$  increases at low fuel mass, reaching a maximum and then decreases when the fuel mass becomes higher while  $b$  keeps climbing with the increasing fuel mass. Generally, the higher the engine speed, the smaller is the value of  $a$  while  $b$  is just the opposite. Fig.8(c) and Fig.8(d) show that generally the value of  $c$  drops at low fuel mass (even below value of 1 which should not be the case since then there would be no combustion anymore) while  $n_{exp}$  rises at low fuel mass. A rising  $n_{exp}$  gets closer to the  $\kappa$  value meaning less heat input (refer to  $Q_{56}$  in Table 2). All in all the late and very late combustion, but also the isobaric combustion tend to become small at low fuel mass input and combustion tends to concentrate in the isochoric stage.

297

### 3.2 Regression polynomials of calculating the combustion parameters

298

299

300

301

302

303

304

In the simulation of the in-cylinder process, the combustion parameters under different operating conditions need to be calculated. In case of the 3-stage combustion, once the isochoric combustion parameter  $a$  and isobaric combustion parameter  $b$  are known, the isothermal combustion parameter  $c$  can be calculated based on the law of energy conservation, assuming that in a (causal) engine simulation model the injected fuel quantity is given. Therefore, only the regression polynomials calculating the isochoric and isobaric combustion parameters are fitted in this paper. It can be observed that when in the basic Seiliger cycle (with three stages of combustion)  $w_i$  is removed as an equivalence criterion (equation 4) but  $T_{max}$  remains to be so, the value of  $a$  and  $b$  do not alter, since they still are fully determined by equation 1 and 2.

305

#### 3.2.1 Fitting of combustion parameters

306

In this paper, the combustion parameters are assumed to be functions of engine speed and fuel mass:

307

$$a = f_a(n_{eng}^{norm}, m_f^{norm}) \quad (7)$$

308

$$b = f_b(n_{eng}^{norm}, m_f^{norm}) \quad (8)$$

309 According to the relationship illustrated in Fig.8(a) and Fig.8(b), the functions of equations (7) and (8) can be written  
 310 in the following forms:

$$311 \quad f_a(n_{eng}^{norm}, m_f^{norm}) = \sum_{i=0}^1 \sum_{j=0}^3 k_{ij}^a (n_{eng}^{norm})^i (m_f^{norm})^j \quad (9)$$

$$312 \quad f_b(n_{eng}^{norm}, m_f^{norm}) = \sum_{i=0}^1 \sum_{j=0}^3 k_{ij}^b (n_{eng}^{norm})^i (m_f^{norm})^j \quad (10)$$

313 The polynomial formulas for calculating the combustion parameters are obtained by using a multivariable regression  
 314 fitting method with the test data and the results are given in Table 7 and Table 8.

315 **Table 7** Fitting results and errors of polynomial calculating isochoric combustion parameter

Polynomial coefficients		SSE	RMSE	R-square
$k_{00}^a$	1.1819			
$k_{01}^a$	1.5726			
$k_{02}^a$	5.7933			
$k_{03}^a$	-6.6553	0.1818	0.0359	0.9675
$k_{10}^a$	-0.3918			
$k_{11}^a$	1.9880			
$k_{12}^a$	-11.5119			
$k_{13}^a$	9.2392			

316 **Table 8** Fitting results and errors of polynomial calculating isobaric combustion parameter

Polynomial coefficients		SSE	RMSE	R-square
$k_{00}^b$	1.0097			
$k_{01}^b$	-0.4124			
$k_{02}^b$	1.2993			
$k_{03}^b$	-1.4407	0.0251	0.0133	0.9693
$k_{10}^b$	0.0076			
$k_{11}^b$	0.3028			
$k_{12}^b$	-0.6847			
$k_{13}^b$	1.2636			

317 Equations (9) and (10) can be written in the following form:

$$\begin{aligned}
a = & 1.1819 + 1.5726m_f^{norm} + 5.7933(m_f^{norm})^2 \\
& - 6.6553(m_f^{norm})^3 - 0.3918n_{eng}^{norm} \\
& + 1.9880n_{eng}^{norm}m_f^{norm} \\
& - 11.5119n_{eng}^{norm}(m_f^{norm})^2 \\
& + 9.2392n_{eng}^{norm}(m_f^{norm})^3
\end{aligned} \tag{11}$$

$$\begin{aligned}
b = & 1.0097 - 0.4124m_f^{norm} + 1.2993(m_f^{norm})^2 \\
& - 1.4407(m_f^{norm})^3 + 0.0076n_{eng}^{norm} \\
& + 0.3028n_{eng}^{norm}m_f^{norm} \\
& - 0.6847n_{eng}^{norm}(m_f^{norm})^2 \\
& + 1.2636n_{eng}^{norm}(m_f^{norm})^3
\end{aligned} \tag{12}$$

### 3.2.2 Verification of the regression polynomials

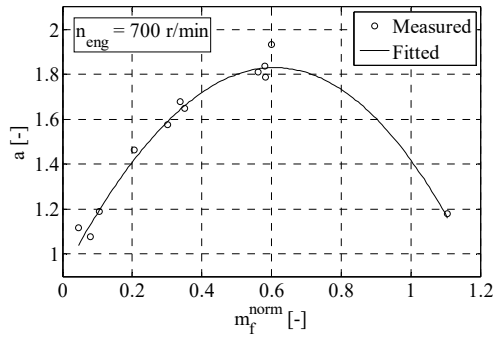
In this part the accuracy of the above regression polynomials are verified by comparing them with the test data and the results are shown in Table 9, Table 10, Fig.9 and Fig.10.

**Table 9** Errors of fitted values and measured values (isochoric combustion parameter  $a$ )

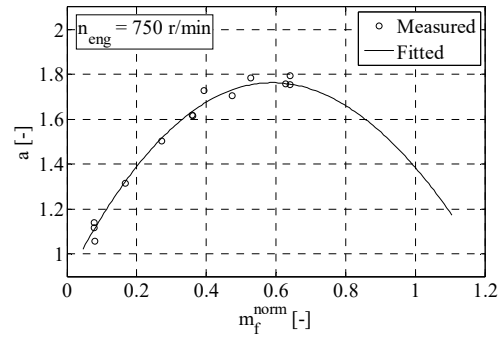
Engine speed [rpm]	SSE	RMSE	R-square
700	0.0254	0.0460	0.9902
750	0.0118	0.0301	0.9338
800	0.0155	0.0312	0.9695
850	0.0193	0.0303	0.9656
900	0.0685	0.0513	0.9057
950	0.0088	0.0191	0.9794
1000	0.0326	0.0335	0.9714

**Table 10** Errors of fitted values and measured values (isobaric combustion parameter  $b$ )

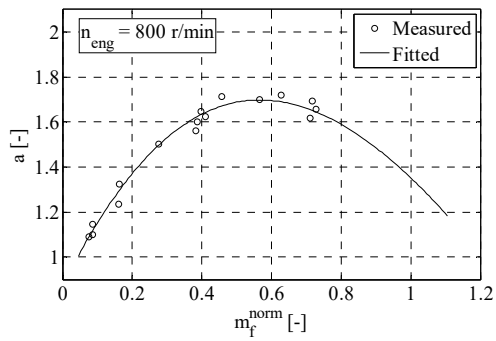
Engine speed [rpm]	SSE	RMSE	R-square
700	0.0254	0.0460	0.9902
750	0.0118	0.0301	0.9338
800	0.0155	0.0312	0.9695
850	0.0193	0.0303	0.9656
900	0.0685	0.0513	0.9057
950	0.0088	0.0191	0.9794
1000	0.0326	0.0335	0.9714



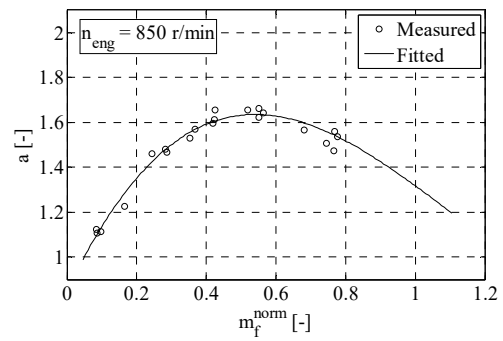
(a) Engine speed 700rpm



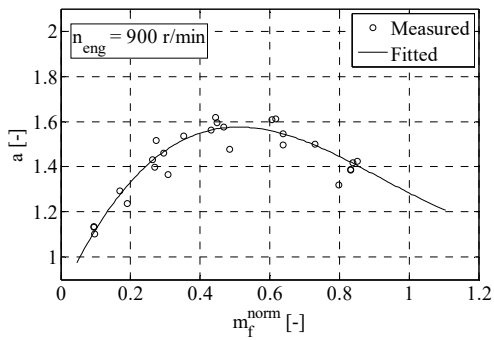
(b) Engine speed 750rpm



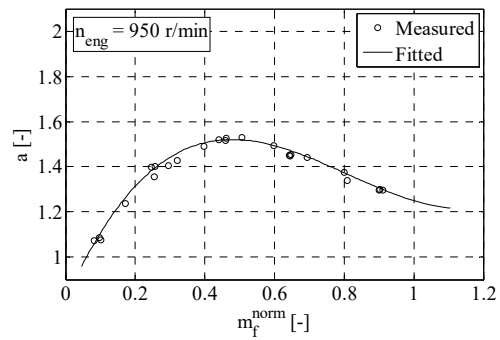
(c) Engine speed 800rpm



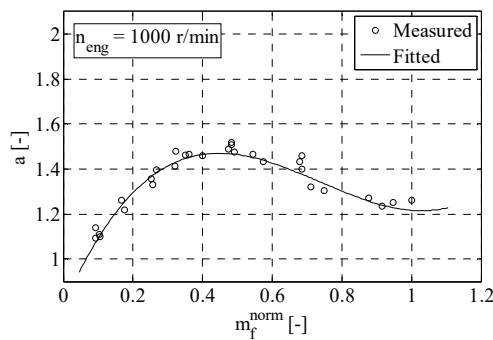
(d) Engine speed 850rpm



(e) Engine speed 900rpm

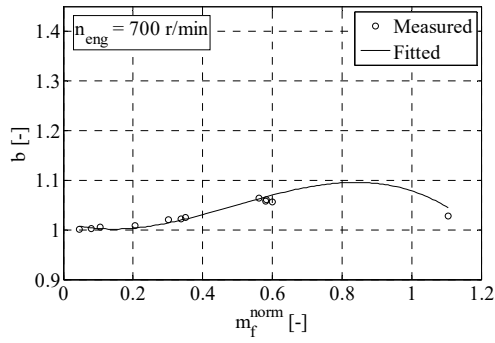


(f) Engine speed 950rpm

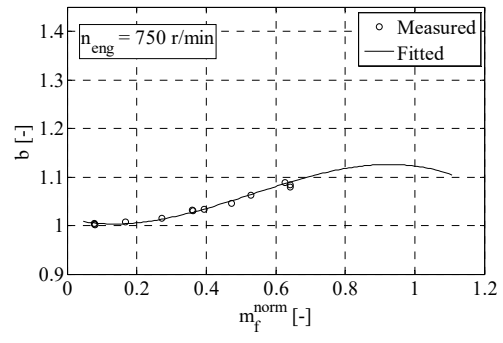


(g) Engine speed 1000rpm

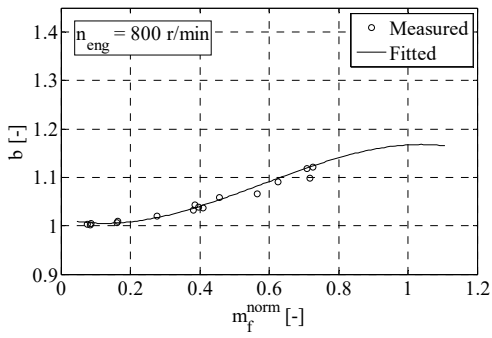
**Fig.9** Comparison of  $a$  between fitted value and test data



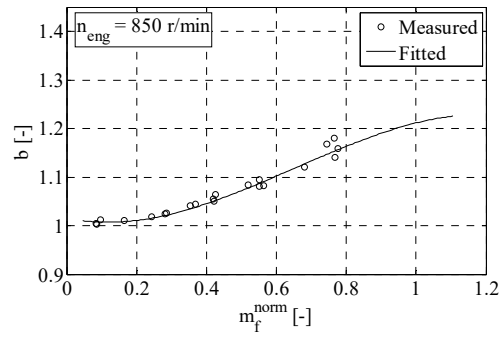
(a) Engine speed 700rpm



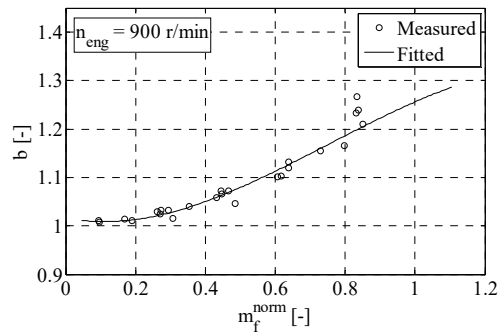
(b) Engine speed 750rpm



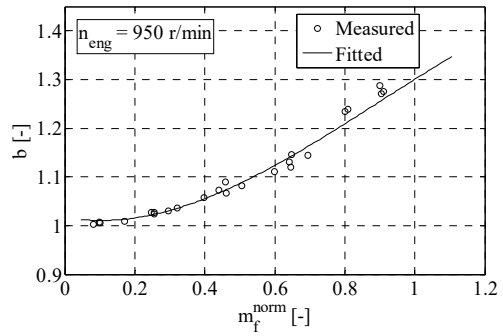
(c) Engine speed 800rpm



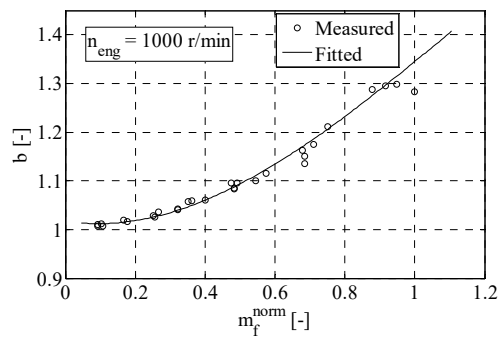
(d) Engine speed 850rpm



(e) Engine speed 900rpm

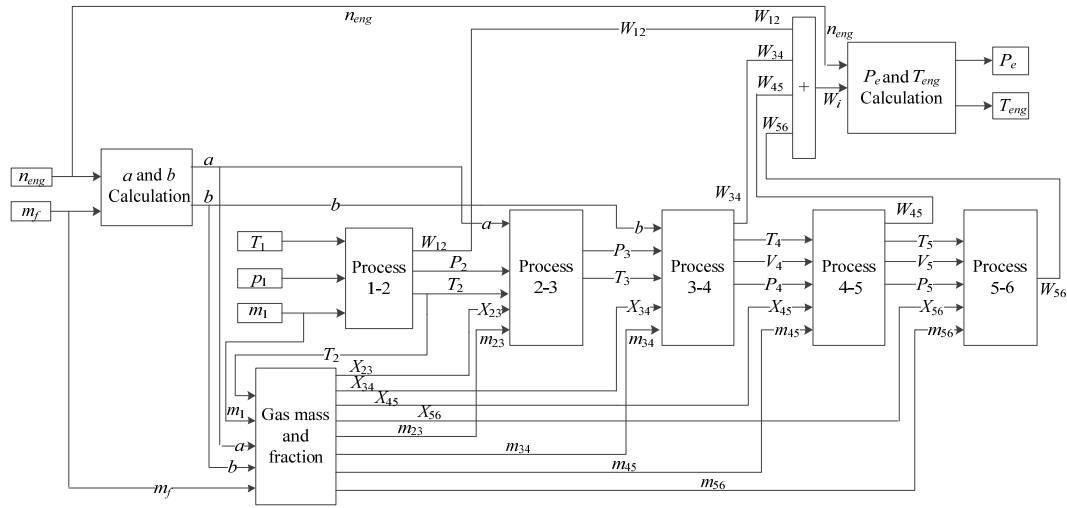


(f) Engine speed 950rpm



(g) Engine speed 1000rpm

**Fig.10** Comparison of  $b$  between fitted value and test data



344  
345 **Fig.11** Mean value model of the in-cylinder process in SIMULINK

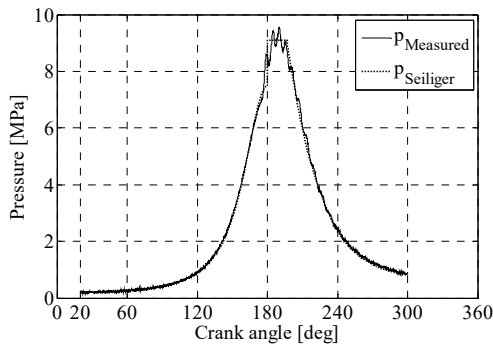
346 **3.3 Mean value model of in-cylinder process in MATLAB/SIMULINK**

347 The mean value model of in-cylinder process built based on the basic six-point Seiliger cycle in  
348 MATLAB/SIMULINK is shown in Fig.11.

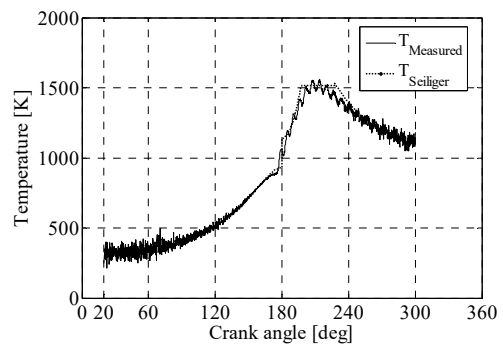
349 In this paper, three different operating points of the in-cylinder process of the MAN 4L20/27 diesel engine are  
350 simulated and the results are shown in Fig.12.

351 The three operating points are as follows:

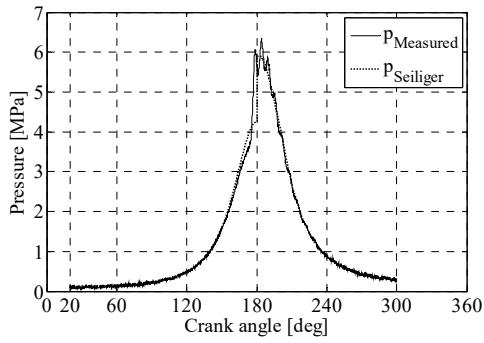
- 352 (A) 1000rpm, 100%  $P_e$  (Nominal engine effective power);
- 353 (B) 1000rpm, 30%  $P_e$ ;
- 354 (C) 800rpm, 50%  $P_e$ .



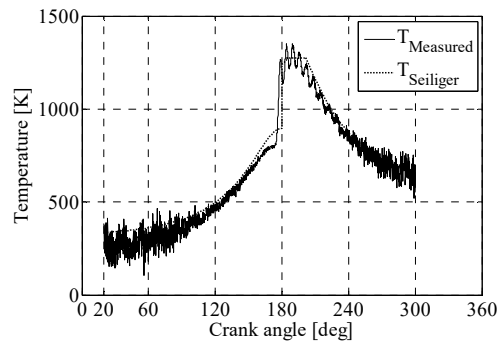
356 (a) In-cylinder pressure (point A)



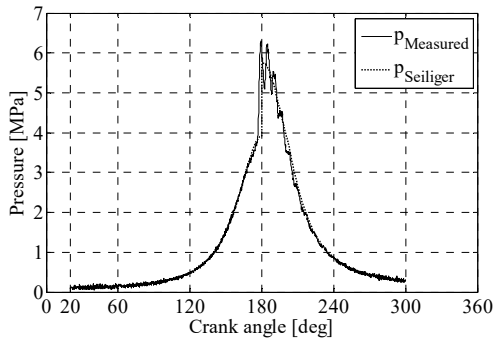
356 (b) Cylinder temperature (point A)



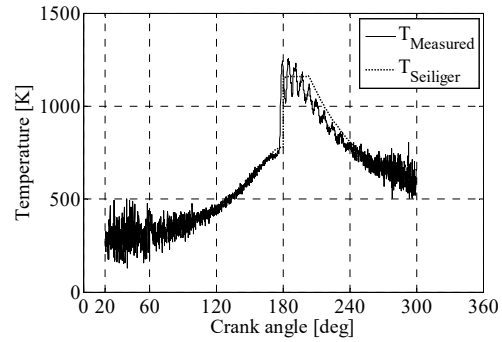
(c) In-cylinder pressure (point B)



(d) Cylinder temperature (point B)



(e) In-cylinder pressure (point C)



(f) Cylinder temperature (point C)

**Fig.12** Comparison of Calculated Seiliger Cycle with test data

If the initial condition (trapped condition) together with the effective compression ratio and the polytropic compression exponent are kept constant, the cylinder pressure and temperature at the end of compression will not change. When the isobaric combustion parameter  $b$  is kept constant, the maximum pressure and maximum temperature in the cylinder will rise with the increase of the isochoric combustion parameter  $a$ . It is obvious that the isochoric combustion parameter  $a$  has a great influence on the maximum pressure and temperature in the cylinder.

When the isochoric combustion parameter  $a$  is kept constant, the maximum in-cylinder pressure will not change with the rising of the isobaric combustion parameter  $b$  while the maximum temperature will keep going up.

It is shown in Fig.12 that the simulation results of the mean value model of the in-cylinder process have a reasonable correspondence with the test data, showing a satisfactory accuracy and adaptability to variable operating conditions.

#### 4 Model application

The mean value diesel engine model presented in previous sections is used in the simulation and performance prediction study of a large semi-submersible heavy lift vessel (SSHLV) propulsion system during the preliminary propulsion system design stage to demonstrate the MVFP engine model can be integrated in a larger system.

The main engine of the propulsion system of SSLV is the diesel engine MAN 18V32/40 connected with a

376 controllable pitch propeller. The main specifications of diesel engine MAN 18V32/40 are reported in Table 11. Since the  
 377 18V32/40 engine is also MAN engine with similar structure (in particular they are both injection systems with plunger  
 378 pumps) as 20/27 engine and they are 4-stroke medium engine with similar working principle, the diesel engine model  
 379 investigated from section 3 based on MAN 20/27 can be used in this diesel engine but with correction. The formulas  
 380 calculating the combustion parameters  $a$  and  $b$  obtained in the previous section are corrected shown in equation (13) -  
 381 (18), making  $p_{max}$  and  $T_{max}$  as the equivalence criteria, before being applied to diesel engine MAN 18V32/40.

$$382 \quad a = a_0 + \Delta a \quad (13)$$

$$383 \quad b = b_0 + \Delta b \quad (14)$$

$$384 \quad p_{max} = p_1 \cdot r_c^{n_{comp}} \cdot a \quad (15)$$

$$385 \quad T_{max} = T_1 \cdot r_c^{n_{comp}-1} \cdot a \cdot b \quad (16)$$

$$386 \quad \Delta a = \frac{p_{max}}{p_1 \cdot r_c^{n_{comp}}} - a_0 \quad (17)$$

$$387 \quad \Delta b = \frac{T_{max}}{T_1 \cdot r_c^{n_{comp}} \cdot a} - b_0 \quad (18)$$

388 Where,  $a_0$ ,  $b_0$  are calculated by equation (11) and (12) respectively.

389 Fig. 13 shows the SIMULINK model of SSSLV propulsion system in which the mean value model of diesel  
 390 engine MAN 18V32/40 is applied. Based on the propulsion system model, both the steady-state behaviour under  
 391 various steady operating conditions and the transient-state performance of the diesel engine have been researched.

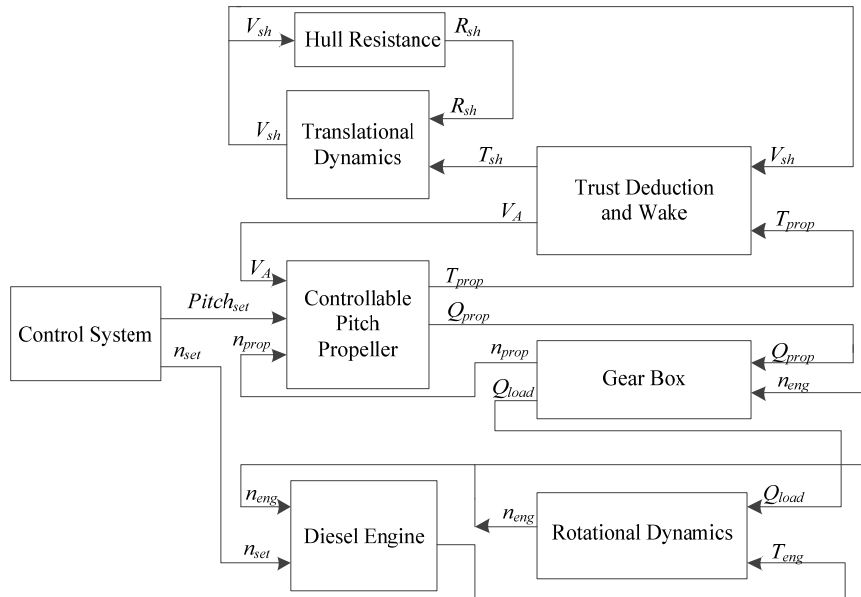
392 **Table 11** Main specifications of Diesel engine MAN 18V 32/40

Parameter	Unit	Value
Nominal Engine Speed	rpm	750
Maximum Effective Power	kW	9000
Cylinder Number	-	18
Bore	m	0.32
Stroke	m	0.40



Compression Ratio	-	14.5
Connecting Rod Ratio	-	0.204
Inlet Valve Close	deg	40°after BDC
Outlet Valve Open	deg	41°before BDC

393



394

395

**Fig. 13** SIMULINK model of SSHLV propulsion system

396

#### 4.1 Steady-state behaviour analysis of SSHLV propulsion system

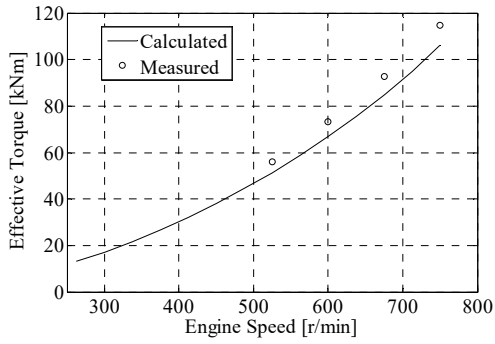
397

The steady-state operating performance of the SSHLV propulsion system under nominal (design) hull resistance condition has been investigated. Various engine performance parameters at different operational speeds under different steady operating conditions are calculated and compared with the diesel engine test data as shown in Fig. 14.

400

The results show that the engine performance parameters, such as the effective torque, mean effective pressure, effective power, effective efficiency, in-cylinder pressure and temperature at IC (inlet close) of the engine, which are calculated by the mean value model are all in reasonable correspondence with the measurements while the calculated specific fuel consumption deviates from the measured data, which could be caused by the estimation of the diesel engine mechanical losses. Mechanical losses are calculated based on Millington model (Millington B W, Hartles E R, 1968) according to which the losses are a function of engine speed and mean piston speed but not on load, while the constants may not be applicable to larger and newer engines. Mechanical losses model will be improved by taking not only engine speed but also load into account in our future work.

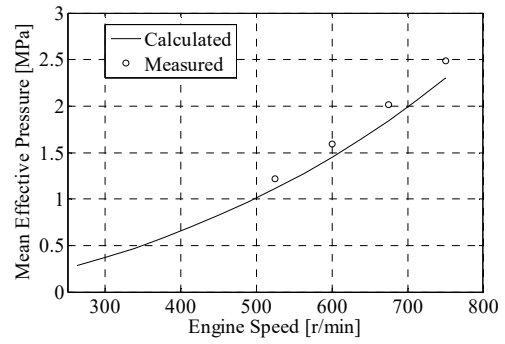
407



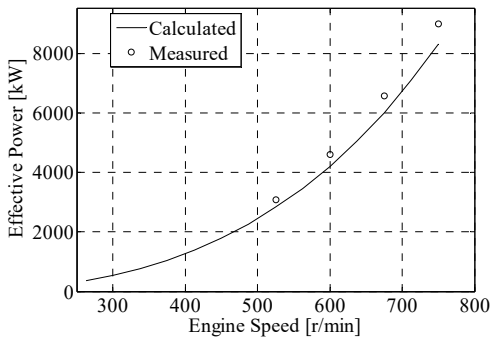
408

409

(a) Effective Torque



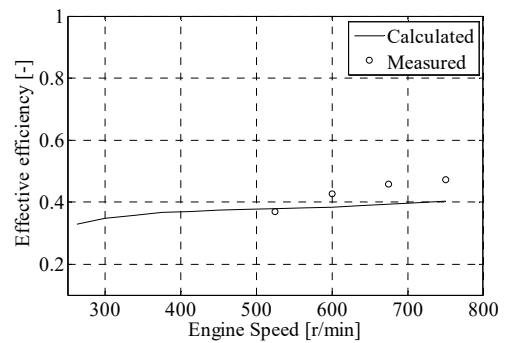
(b) Mean Effective Pressure



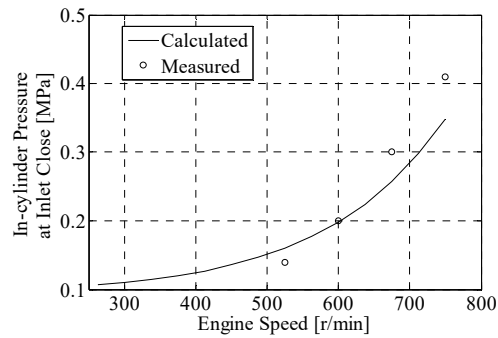
410

411

(c) Effective Power



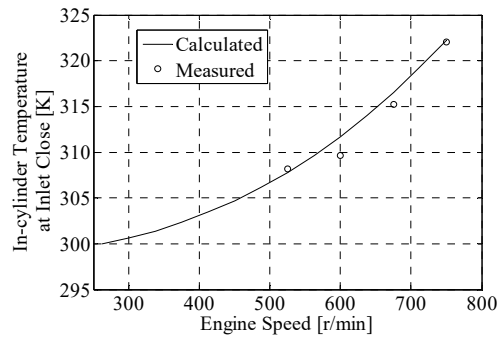
(d) Effective Efficiency



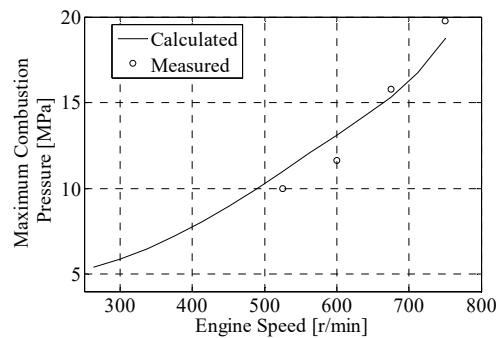
412

413

(e) In-cylinder Pressure at IC



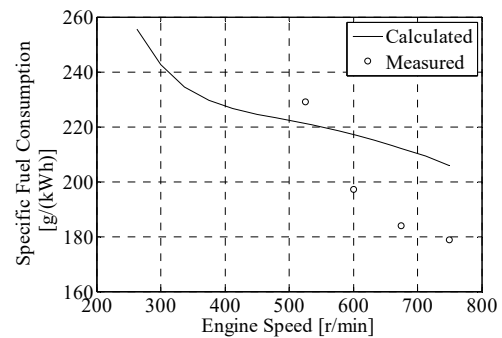
(f) In-cylinder Temperature at IC



414

415

(g) Maximum Combustion Pressure



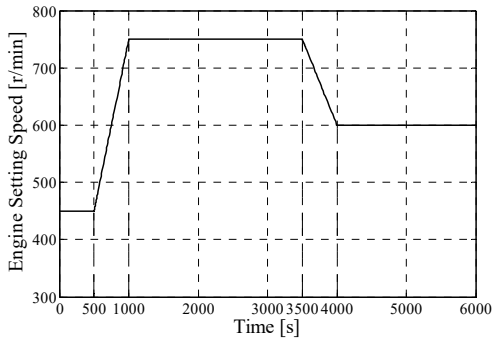
(h) Specific Fuel Consumption

416

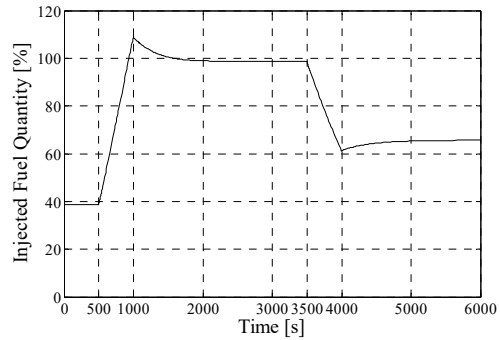
**Fig. 14** Comparison of calculated steady-state engine performance parameters with test data

417 **4.2 Transient-state behaviour analysis of SSHLV propulsion system**

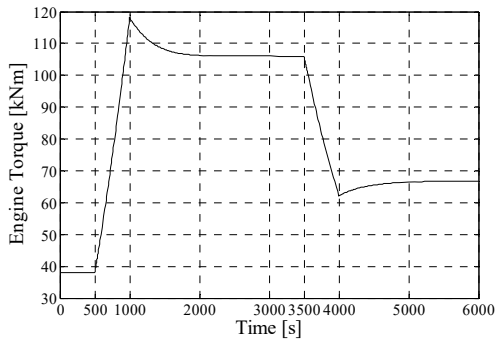
418 The MAN 18V32/40 diesel engine mean value model has been used for a transient-state performance analysis of  
 419 the SSHLV propulsion system. The transient-state behaviour of the ship propulsion system under both acceleration and  
 420 deceleration operating conditions by changing the engine operational speed has been predicted and investigated. The  
 421 simulation time is set 6000 seconds long and the engine speed of 450 rpm is set as the initial engine operation state  
 422 when the ship moves forward at speed of 8.66 knots. The details of engine speed setting command are illustrated in Fig.  
 423 15(a). The propulsion system operates at initial steady state over 0s~500s. The engine speed increases linearly from  
 424 450rpm to 750rpm during 500s~1000s. From 1000s to 3500s, the setting engine speed is kept at 750rpm. The engine  
 425 speed setting decreases linearly from 750rpm to 600rpm and then is maintained until 6000s. The engine transient  
 426 behaviour during the acceleration and deceleration operational process has been presented in Fig. 15(b) to Fig. 15(g).



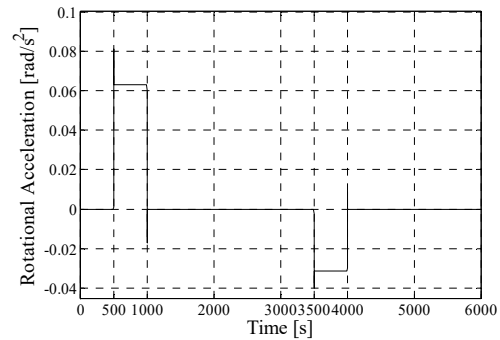
427  
428 (a) Engine Setting Speed



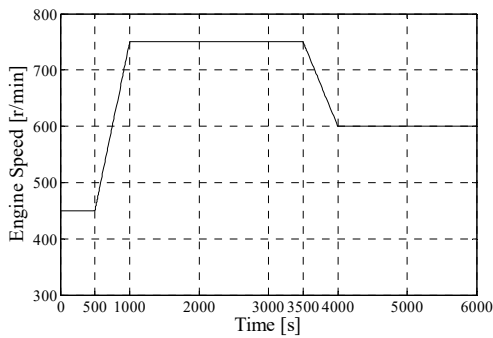
429 (b) Injected Fuel Quantity



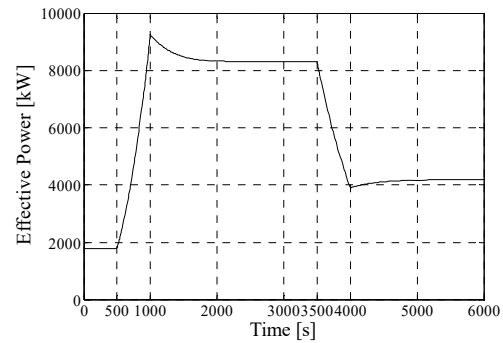
430 (c) Engine Torque



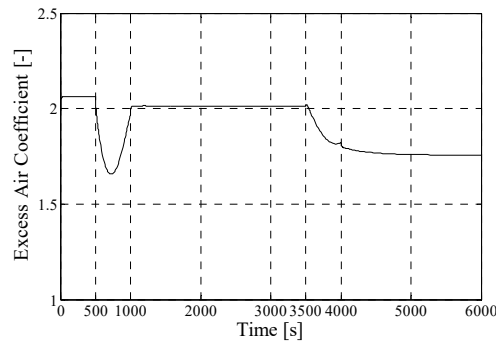
431 (d) Rotational Acceleration



(e) Engine Speed



(f) Effective Power



(g) Excess Air Coefficient

**Fig. 15** Engine transient behaviour during operational process

## 5 Conclusions

In this paper a Mean Value First Principle (MVFP) modelling method for diesel engines, based on both the basic and advanced six-point Seiliger cycle in which the in-cylinder process is characterized using the parameterized finite stages, has been investigated. The mean value model of the MAN 4L20/27 diesel engine has been analysed using an advanced Seiliger cycle that proved to be capable of correctly representing the late and very late combustion seen in this older engine.

For more modern engines with high-pressure injection systems it seems allowed to use the basic six-point Seiliger cycle for making an engine simulation model. The formulas calculating the isochoric combustion parameter and isobaric combustion parameter in this model are fitted using multivariable regression fitting method with the experimental data. The isothermal combustion parameter is calculated according to the law of energy conservation.

The resulting mean value diesel engine model has been adapted to a larger and modern MAN 18V32/40 engine and the results of this model are compared to test data and show reasonable correspondence although there is room for improvement, as reported in this paper. Finally this engine model has been used in a simulation and performance prediction study of the propulsion system of an SSHLV under both steady and transient operational conditions.

451 The MVFP model as developed in this paper is able to generate the overall engine parameters such as the  
452 in-cylinder pressure and temperature etc. quickly in a satisfactory accuracy. The simulation results have shown the  
453 adaptability of the MVFP model to variable working conditions and the capability of being integrated into a large  
454 system. It's applicable to both steady-state and transient-state simulation and performance prediction of a large ship  
455 propulsion system.

456 The modelling approach used in this paper is not only valid for diesel engines but in principle also valid for both Otto cycle  
457 engines and gas engines. For Otto cycle engines, if both the isochoric and the isothermal combustion parameters are equal to  
458 unity, the cycle will become the Otto process. When it comes to gas engines it has been found that as for the diesel process the  
459 6-point Seiliger cycle must be used, however with very different values for the isochoric and isobaric combustion parameters  
460 (Georgescu I, et al., 2016). Also other adaptations must be made before the modelling method can be applied to modelling gas  
461 engines (amongst other the fact that gas as a fuel does not require heat for evaporating) and that will be presented in our future  
462 work.

## 463 **Acknowledgement**

464 This project partly is financially supported:

- 465 1. International Science & Technology Cooperation Program of China, 2014DFG72360.
- 466 2. Scientific Research Foundation for the Returned Overseas Chinese Scholars, State Education Ministry.
- 467 3. China Scholarship Council, grant number 201606680010.

## 468 **References**

- 469 Lino Guzzella and Christopher H. Onder., 2010. Introduction to modeling and control of internal combustion engine systems.  
470 Berlin: Springer-Verlag.
- 471 Asprion, J., et al., 2013. A fast and accurate physics-based model for the NOx emissions of Diesel engines. Applied Energy  
472 103: 221-233.
- 473 Chung J, Oh S, Min K and Sunwoo M., 2013. Real-time combustion parameter estimation algorithm for light-duty diesel  
474 engines using in-cylinder pressure measurement. Applied Thermal Engineering, 60: 33-43.
- 475 Rakopoulos, C. D., Giakoumis, E. G., 2006. Review of thermodynamic diesel engine simulations under transient operating  
476 conditions. Sae Technical Papers, 115.
- 477 Guan, C., Theotokatos, G., Zhou, P. L., Chen, H., 2014. Computational investigation of a large containership propulsion  
478 engine operation at slow steaming conditions. Applied Energy 130: 370-383.

479 Payri, F., et al., 2011. A complete 0D thermodynamic predictive model for direct injection diesel engines. *Applied Energy*  
480 88(12): 4632-4641.

481 Woodward J B, Latorre R G, 1984. Modeling of diesel engine transient behavior in marine propulsion analysis.  
482 *Transactions-Society of Naval Architects and Marine Engineers*.92:33-49.

483 Theotokatos G, 2010. On the cycle mean value modelling of a large two-stroke marine diesel engine. *Proceedings of the*  
484 *Institution of Mechanical Engineers, Part M: Journal of Engineering for the Maritime Environment*, **224**(3):193-205.

485 Murphy, A. J., et al., 2015. Thermodynamic simulation for the investigation of marine Diesel engines. *Ocean Engineering* 102:  
486 117-128.

487 Moskwa, J. J., & Hedrick, J. K., 1992. Modeling and validation of automotive engines for control algorithm development.  
488 *Journal of Dynamic Systems Measurement & Control*, 114(2), 278-285.

489 Kao, M., and Moskwa, J., 1995. Turbocharged diesel engine modelling for nonlinear engine control and state estimation.  
490 *Journal of Dynamic Systems Measurement & Control*, 117(1), 20-30.

491 Maftai, C., Moreira, L., Soares, C. G., 2009. Simulation of the dynamics of a marine diesel engine. *Proceedings of the*  
492 *Institute of Marine Engineering Science & Technology Part A Journal of Marine Engineering & Technology*, 2009(15),  
493 29-43.

494 Lee B, Jung D, Kim Y W, et al., 2013. Thermodynamics-Based Mean Value Model for Diesel Combustion. *Journal of*  
495 *Engineering for Gas Turbines & Power*, 135(9):942-955.

496 Miedema, S. and Z. Lu., 2002. The dynamic behaviour of a diesel engine. *Proceedings of the WEDA XXII technical*  
497 *conference and 34th Texas A&M dredging seminar, Denver, Colorado, USA.*

498 Baldi, F., et al., 2015. Development of a combined mean value-zero dimensional model and application for a large marine  
499 four-stroke Diesel engine simulation. *Applied Energy* 154: 402-415.

500 Schulten P J M, 2005. The interaction between diesel engines, ship and propellers during manoeuvring. Ph.D thesis, Delft  
501 University of Technology, Delft.

502 Grimmelius, H., Mesbahi, E., Schulten, P., & Stapersma, D., 2007. The use of diesel engine simulation models in ship  
503 propulsion plant design and operation. *CIMAC International Council on Combustion engines*, 1-12.

504 M Martelli, 2014. *Marine Propulsion Simulation*. PhD thesis, Genoa University, Italy.

505 Altosole, M. and M. Figari., 2011. Effective simple methods for numerical modelling of marine engines in ship propulsion  
506 control systems design. *Journal of Naval Architecture and Marine Engineering* 8(2).

507 Theotokatos, G. P., 2008. Ship propulsion plant transient response investigation using a mean value engine model.  
508 *International Journal of Energy*, 2: 66-74.

509 Vrijdag A, Stapersma D and van Terwisga T, 2010. Control of propeller cavitation in operational conditions. *Journal of*  
510 *Marine Engineering and Technology*, A16: 15-26.

511 Ding Y, 2011. *Characterising Combustion in Diesel Engines: using parameterised finite stage cylinder process models*. PhD  
512 thesis, TU Delft, The Netherlands.

513 Heywood, J., 1988. *Internal combustion engine fundamentals*. New York, McGraw-Hill.

514 Lapuerta, M., et al., 2006. Effect of the gas state equation on the thermodynamic diagnostic of diesel combustion. *Applied*  
515 *Thermal Engineering* 26(14): 1492-1499.

516 Stapersma D, Klein Woud H, 2002. *Design of propulsion and electric power generation systems*. Institute Of Marine  
517 Engineering S A T U, London (United Kingdom): IMarEST.

518 Woschni, G., 1967. A universally applicable equation for the instantaneous heat transfer coefficient in the internal combustion  
519 engine. SAE paper no. 670931.

520 Ding Y, Stapersma D and Grimmelius H. T., 2011. A new method to smooth the in-cylinder pressure signal for combustion  
521 analysis in diesel engines. *Proc. Inst. Mech. Eng., Part A* 225 (3): 309–318.

522 Ding, Y., et al., 2012. Using Parametrized Finite Combustion Stage Models to Characterize Combustion in Diesel Engines.  
523 *Energy & Fuels* 26(12): 7099-7106.

524 Millington B W, Hartles E R, 1968. Frictional losses in diesel engines. SAE Technical Paper, No. 680590.

525 Georgescu I, Stapersma D and Mestemaker B., 2016. Dynamic Behaviour of Gas and Dual-Fuel Engines: Using Models and  
526 Simulations to Aid System Integration. In 28th CIMAC World Congress on Combustion Engine (Paper No. 126).